

ELECTRICAL RESISTANCE AND MAGNETORESISTANCE OF HIGHLY ORIENTED AND POLYCRYSTALLINE $\text{La}_{0.67}\text{Sr}_{0.33}\text{MnO}_3$ / $\text{MgO}(001)$ THIN FILMS

B. Vengalis^a, I. Čerņiukė^a, A. Maneikis^a, A.K. Oginskis^a,
and G. Grigaliūnaitė-Vonševičienė^b

^a Center for Physical Sciences and Technology, A. Goštauto 11, LT-01108 Vilnius, Lithuania

^b Vilnius Gediminas Technical University, Saulėtekio 11, LT-10223 Vilnius, Lithuania

E-mail: veng@pfi.lt

Received 6 February 2015; revised 28 February 2015; accepted 15 June 2015

$\text{La}_{0.67}\text{Sr}_{0.33}\text{MnO}_3$ thin films exhibiting a highly (001)-plane oriented and polycrystalline structure with a variable amount of (011)-textured crystallites have been grown *in situ* by RF magnetron sputtering on crystalline $\text{MgO}(001)$ substrates by changing deposition temperature from 550 to 800 °C. Competing contribution of grains and grain boundaries to resistivity and magnetoresistance of the films has been investigated at $T = (78\text{--}330)$ K. A model based on two parallel channels of current flow across grain boundaries has been applied to explain coexistence of low (LFMR) and high field (HFMR) magnetoresistance effects in the polycrystalline films at low temperatures. The LFMR effect has been understood assuming tunnelling of spin-polarized carriers via magnetic field-driven tunnelling barriers formed naturally between neighbouring misoriented grains. Meanwhile, the HFMR phenomenon has been associated with magnetic field-dependent hopping of carriers via the intergrain regions with reduced carrier density. Importance of the phase separation phenomenon on possible inhomogeneity of the material at grain boundaries has been discussed.

Keywords: LSMO thin films, grain boundaries, electrical resistivity, low field magnetoresistance

PACS: 73.43 Qt, 73.61-r, 71.30.+h, 75.70

1. Introduction

Lanthanum manganites referred to as $\text{La}_{1-x}\text{A}_x\text{MnO}_3$ ($\text{A}=\text{Ca}, \text{Sr}, \text{Ba}$) are attractive due to the paramagnetic-ferromagnetic (PM-FM) phase transition and the large so-called colossal magnetoresistance (CMR) observed in the vicinity of the Curie temperature T_C . CMR is an intrinsic effect originating from double exchange between neighbouring manganese ions. Strontium-doped manganite, $\text{La}_{0.67}\text{Sr}_{0.33}\text{MnO}_3$ (LSMO), exhibiting the highest T_C value (~ 350 K) among the member compounds, provides special interest for room temperature applications although operation of the devices based on the CMR effect in high crystalline quality material is limited due to a relatively strong magnetic field ($\mu_0 H > 1.0$ T) and a narrow temperature range just below T_C [1, 2].

During the last years, increasing attention has been paid to polycrystalline manganites demonstrating a significant grain boundary-governed (extrinsic) magnetoresistance at low fields. The low field

magnetoresistance (LFMR) values up to about 30% have been measured for bulk ceramics and thin films at relatively low magnetic fields ($\mu_0 H < 0.1$ T) and low temperatures ($T \ll T_C$) where the CMR ratios are vanishingly small for single crystals or epitaxial films of the same composition [1–5]. Investigation of single grain boundaries (GBs) formed by growing the manganite films on bicrystal substrates revealed gradual decrease of the LFMR values with temperature increasing up to T_C . Clearly defined nonlinear current–voltage (I – V) relations have been reported additionally for the device structures containing the artificially formed GBs [6–9].

In addition to the LFMR phenomenon, polycrystalline manganites demonstrate magnetoresistance at high magnetic fields (HFMR). In contrast to the intrinsic CMR effect, significant HFMR values were indicated in the whole temperature range below T_C [1–3]. A great number of bulk ceramic samples, polycrystalline thin films, step edge junctions and single artificial GBs have been investigated although

the origin of complex magnetotransport phenomena in polycrystalline manganites is still under debate [1–3, 10, 11].

Tunnelling of spin-polarized carriers across the GBs described by the well-known Julliere theory [12] has been proposed to explain the LFMR phenomenon in polycrystalline manganites [9, 13]. The origin of tunnel barrier has been associated with the band bending effect due to the suppressed magnetic order close to GBs [7]. The observed nonlinear I – V behaviour of a single GB has been understood taking into account additional tunnelling of carriers across an insulating barrier containing high density of localized defect states [2, 6, 7]. However, significant magnetoresistance of polycrystalline manganites at high fields (HFMR) cannot be accounted for by applying the proposed tunnelling model.

The alternative theories, i. e. the mesoscopic media model based on hopping of carriers in the GB region polarized by the adjacent magnetically soft grains [14] and the model based on spin-dependent scattering of carriers at the edges of ferromagnetic grains [5], have been used also to explain the LFMR effect. Note, however, that nonlinear I – V characteristics reported for the artificial junctions cannot be explained within these models. There were also attempts to explain magnetoresistance at high external magnetic fields. The HFMR in polycrystalline manganites has been associated with the evolution of band structure at GBs taking into account the magnetic field-driven barrier height [15, 16]. The HFMR effect in polycrystalline LSMO films grown on polycrystalline Al_2O_3 substrates has been modeled by applying a modified Mott's hopping transport and assuming that GBs might be ferromagnetic with reduced Currier temperature T_c in respect to that of grains [17].

A concept based on a nonuniform current flow across the GBs has been carried out by a number of authors to explain the enhanced resistivity and complex magnetotransport properties in polycrystalline manganites [18, 19] and single GBs. A two-channel model with current flowing via perfect interconnections between grains exhibiting metallic conductivity and those exhibiting poor connectivity has been suggested [18] although the origin of nonuniform current flow via GBs has not yet been fully understood. There is still a great need to study complex magnetotransport properties of polycrystalline manganites taking into account different microstructure and preparation conditions of various systems and particularly thin films. Certainly, GBs in bulk ceramics and thin films are usually formed under different technological conditions. The crys-

talline quality and grain size of bulk ceramics may be tuned by varying either the synthesis temperature or annealing duration while the microstructure of thin films is usually defined by deposition temperature, T_s , crystallinity of a substrate and possible lattice mismatch. The key importance of T_s for crystallinity and magnetotransport properties has been pointed out recently for the LSMO films grown on lattice-mismatched YSZ substrates [9].

The goal of this work was to investigate possible variation of magnetotransport properties of (001)-plane textured LSMO thin films when grown by RF magnetron sputtering on single crystal MgO(001) substrates exhibiting significant lattice mismatch (of about 8.0%) in respect to the film material. It was found that the amount of (001)-plane mis-oriented grains may be tuned in a controlled manner by changing substrate temperature in the range 550–800 °C. Grain boundary-governed magnetotransport properties of the grown films, i. e. temperature dependent enhanced resistivity as well as the LFMR and HFMR effects, were investigated for various films in a wide temperature range below T_c . Variation of the observed magnetotransport properties has been analyzed within the framework of the existing phenomenological models.

2. Experiment

The LSMO films were grown *in situ* on cleaved (001) faces of a cubic MgO single crystal ($a_c \cong 0.421$ nm) by radio frequency magnetron sputtering of a disk-shaped ceramic target with a diameter of 25 mm and chemical composition $\text{La}_{0.67}\text{Sr}_{0.33}\text{MnO}_3$. The Ar- O_2 (1:1) gas mixture with partial oxygen pressure of about 15 Pa was used for sputtering. During deposition, the substrates were kept at fixed temperatures ranging from 550 to 800 °C. After the deposition, all the films were cooled down slowly to room temperature under oxygen pressure of about 5×10^4 Pa to fully saturate the films by oxygen. Hereafter in the text, the films are marked according to their deposition temperatures 500–800 °C by L500–L800, respectively.

The thickness of the prepared films measured by a DEKTAK 6M profilometer ranged typically from 150 to 200 nm. The growth rate of the films was 2–3 nm/min. The crystalline structure of the films was investigated by measuring X-ray diffraction patterns in Θ – 2Θ geometry using CuK_α radiation. Surface morphology of the grown films was investigated by a scanning probe atomic force microscope (AFM) Dimension 3100 (*Digital Instruments*) operating in a tapping mode regime.

Stripe-like films with typical square dimensions ($1.5 \times 7.0 \text{ mm}^2$) were used for electrical measurements. Electrical resistance and magnetoresistance defined as $MR = [R(H) - R(0)]/R(0)$ were measured in a wide temperature range ($T = 78\text{--}350 \text{ K}$) by applying the four-probe method and using DC current of 0.1 mA.

3. Results

Typical Θ - 2Θ XRD scans measured for the L800 and L600 films are shown in Fig. 1. Clearly defined (001) and (002) XRD patterns seen for the L800 film certify highly oriented oxide material with crystallographic planes of (001) type oriented parallel to the film plane. Meanwhile, relatively weak additional (011) XRD reflexes have been indicated for the films grown at 750 °C and lower temperatures. Intensity of these reflexes was found to increase with substrate temperature decreasing although the (001) texture has been indicated as dominating for all the grown films. The out-of-plane lattice parameter of a pseudocubic unit cell, a_c , of about 0.3875 nm estimated for the highly textured L800 film from the (002) reflection patterns is in good coincidence with that indicated for the bulk material of the same composition. It means that the lattice strain caused by the MgO substrate was nearly relaxed in the films. Slightly higher a_c value (of about 0.3890 nm) indicated in this work for the L550 film may, probably, be associated with increased density of point defects due to relatively low film growth temperature.

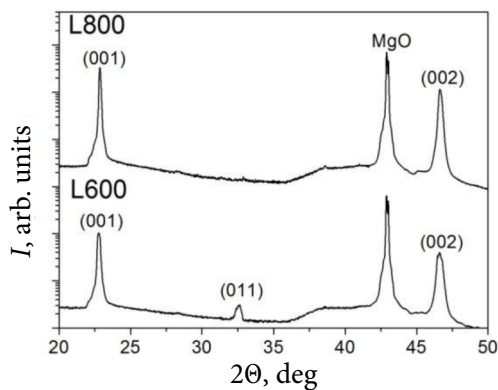


Fig. 1. Θ - 2Θ XRD reflexes measured for the L800 and L600 films grown on MgO(001) substrates at 800 and 600 °C, respectively.

Typical AFM surface images of two LSMO films grown on MgO substrates at 800 and 600 °C are displayed in Fig. 2(a, b). The averaged surface roughness of the films ranged from 2.51 nm for the L800 film to about 4.22 nm for the L550 film.

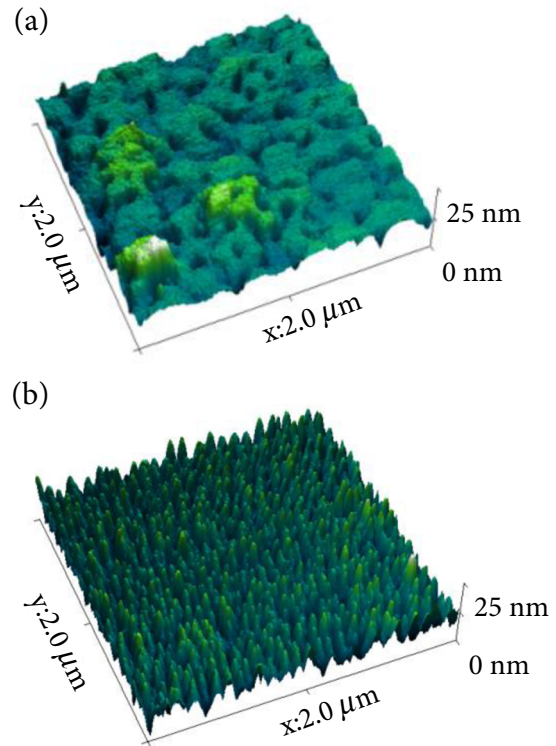


Fig. 2. AFM surface images of the L800 and L600 films grown on MgO(001) substrates at 800 (a) and 600 °C (b).

The averaged grain size estimated for various films was found to decrease from about 286 to 45 nm with substrate temperature, T_s , decreasing from 800 to 550 °C (see Table 1).

Table 1. Thickness d_p , average roughness R , and grain size d_G of the LSMO films grown at different substrate temperatures T_s , as found from AFM surface images.

T_s , °C	800	750	700	650	600	550
d_p , nm	210	180	220	215	195	160
R , nm	2.51	2.83	2.60	3.2	3.95	4.22
d_G , nm	286	133	95	69	57	45

Resistivity versus temperature, $\rho(T)$, of the LSMO films grown on MgO(001) substrates at different temperatures ($T_s = 550\text{--}800 \text{ °C}$) is shown in Fig. 3(a). The measured $\rho(T)$ dependence of the highly oriented L800 film seen in the figure is typical for the highest quality epitaxial LSMO films when grown on SrTiO₃ or other lattice-matched crystalline substrates [2]. The characteristic resistance peak seen for the film at $T = T_p \approx 330 \text{ K}$ and significant ρ decrease with T decreasing from T_p down to about 270 K are a result of a paramagnetic insulator to ferromagnetic metal transition at the Curie temperature $T_c \cong T_p$ while almost linear ρ decrease with temperature lowering

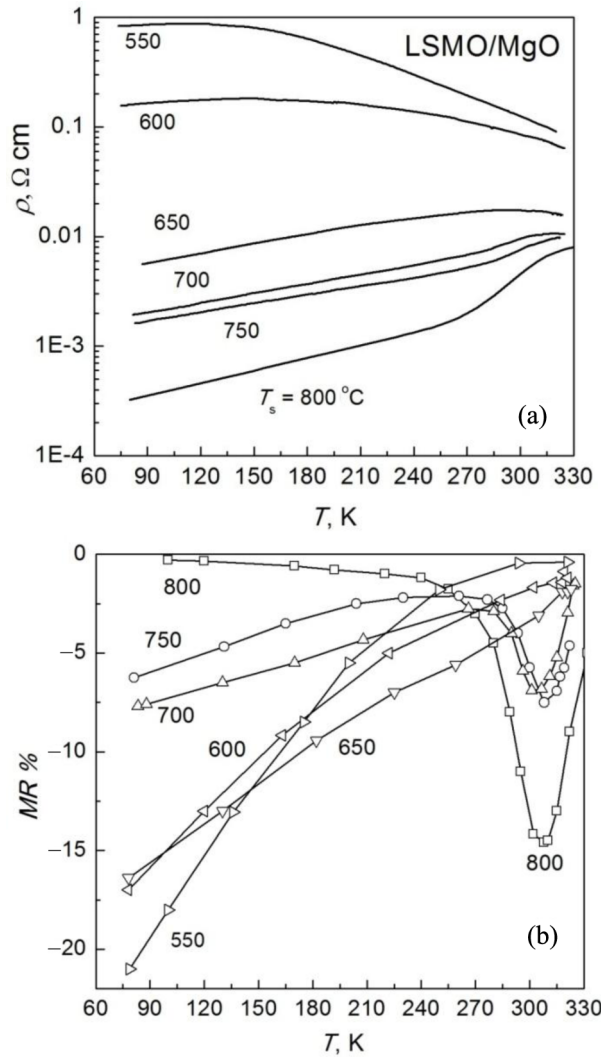


Fig. 3. Resistivity (a) and magnetoresistance ($\mu_0 H_{\parallel} = 0.73$ T) (b) vs temperature measured for the LSMO films grown on MgO substrates at different temperatures, $T_s = 550$ – 800 °C. Lines in Fig. 3(b) are guides for an eye.

from 270 K down to 78 K is defined by temperature-dependent scattering process [20].

In Fig. 3(a) one can notice that ρ values of all polycrystalline LSMO films in the whole temperature range are significantly higher compared to that of the highly oriented L800 film. Gradual increase of ρ with T_s decreasing from 800 to 550 °C demonstrate an increasing role of grain boundaries on resistivity of the grown polycrystalline films [2, 3].

Magnetoresistance, $MR = [R(H) - R(0)]/R(0)$, measured for the same films at a fixed magnetic field ($\mu_0 H_{\parallel} = 0.73$ T) applied parallel to a film plane, is shown in Fig. 3(b). Following Fig. 3(b) we point out peak-like $MR(H)$ anomalies with the highest negative MR of about 14% measured at $T = 305$ K for the highest crystalline quality L800 film. Polycrystalline films grown at 750, 700 and 650 °C showed similar $MR(T)$

anomalies with reduced peak amplitudes while negligibly small MR values have been measured in the same temperature range for the films grown at low temperatures ($T_s = 600$ and 550 °C).

In contrast, highly resistive polycrystalline L550 and L600 films demonstrated the highest MR values at low temperatures while a rather small negative MR value ($\leq 0.2\%$) has been measured at 78 K for the highly oriented L800 film.

Figure 4 shows MR of the highly oriented L800 film and polycrystalline L650 film measured at $T = 300$ K as a function of magnetic field applied parallel (H_{\parallel}) and perpendicular (H_{\perp}) to a film plane (see solid and open points in Fig. 4, respectively). Significant MR anisotropy seen for the films in Fig. 4 can be attributed to shape-related magnetisation anisotropy [21, 22]. Higher negative magnetoresistance MR_{\parallel} values measured by applying magnetic field parallel to a film plane certify that easy axis of magnetization should be parallel to a film plane.

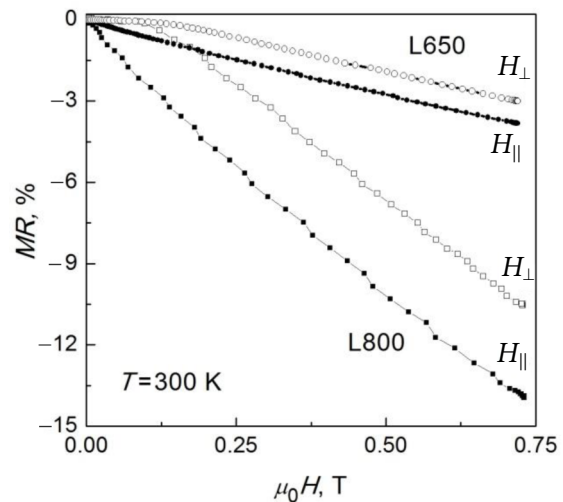


Fig. 4. Magnetic field-dependent magnetoresistance measured for the L800 and L650 films at 300 K.

MR of the highly oriented L800 film and polycrystalline L750, L650, L550 films measured at 78 K as a function of magnetic field applied parallel (H_{\parallel}) and normal (H_{\perp}) to a film plane is displayed in Fig. 5(a, b, c). In the figure we point out the following: 1) clearly defined peak-like $MR(H)$ anomalies at low magnetic fields ($\mu_0 H < 0.25$ T); 2) significant hysteresis of the $MR(H)$ curves; 3) MR anisotropy with applying magnetic field parallel and normal to a film plane; and 4) almost linear $MR(H)$ behaviour for all the films at high magnetic fields ($\mu_0 H > 0.25$ T).

It is important to note that the characteristic $MR(H)$ peaks observed for all polycrystalline LSMO films at low magnetic fields decreased gradually with

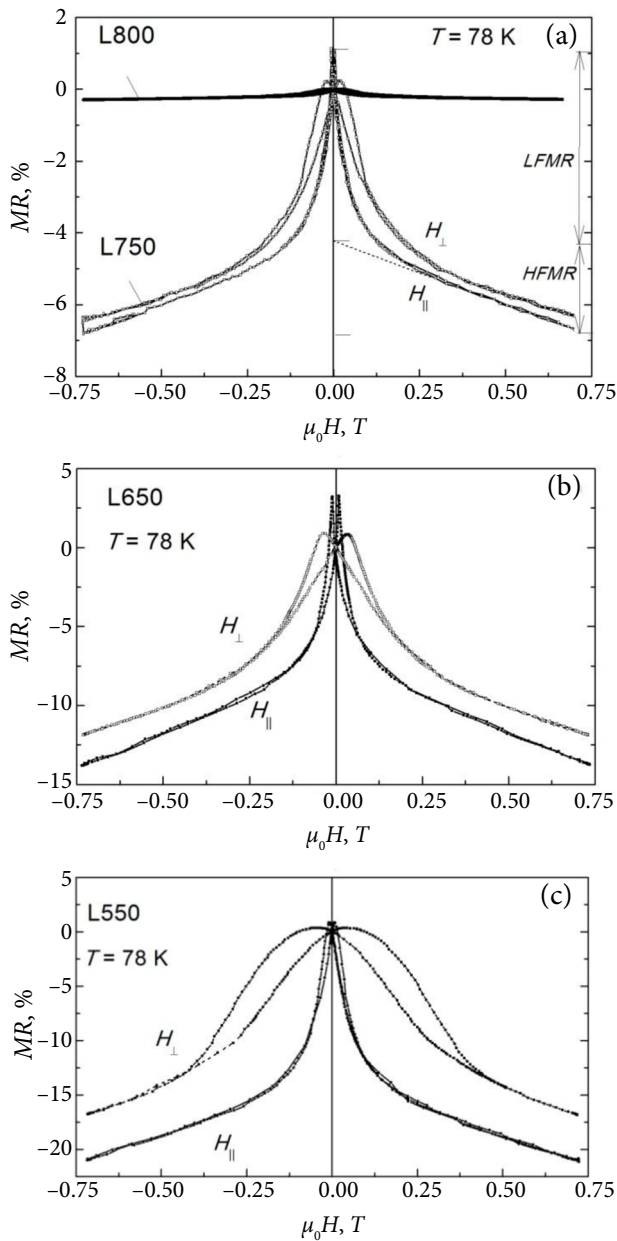


Fig. 5. Magnetic field-dependent magnetoresistance measured at 78 K for the highly oriented L800 film (a) and polycrystalline L750 (a), L650 (b), L550 (c) films. Magnetic field was applied parallel (H_{\parallel}) and normal (H_{\perp}) to a film plane.

temperature increasing from 78 K up to 300 K (see the $MR(H)$ dependence in Fig. 4 measured for the L650 film at 300 K). Similar peak-like $MR(H)$ behaviour at low magnetic field known as low field magnetoresistance (LFMR) has been reported earlier both for polycrystalline ceramics and thin films [1–4].

The LFMR values have been defined in this work as a difference between the MR peak values corresponding to the coercive field $H_{c\parallel}$ and those obtained by extrapolating linear $MR(H)$ slopes (at high field) to the corresponding zero field values (see Fig. 5(a)).

The MR peak values have been associated with the zero magnetisation state at the characteristic coercive fields, $H_{c\parallel}$ [1–4]. Major parameters, namely, magnetoresistance of the films, $MR_{\parallel}(305\text{ K})$, measured at $\mu_0 H_{c\parallel} = 0.73\text{ T}$, $LFMR_{\parallel}(78\text{ K})$, $HFMR_{\parallel}(78\text{ K})$ at $\mu_0 H_{\parallel} = 0.73\text{ T}$, and the coercive fields, $H_{c\parallel}(78\text{ K})$, corresponding to the MR maxima are displayed in Table 2.

Table 2. Magnetoresistance $MR_{\parallel}(305\text{ K})$, measured at 305 K ($\mu_0 H_{\parallel} = 0.73\text{ T}$) and $MR_{\perp}^*(305\text{ K})$ estimated from (2), $LFMR_{\parallel}$ and $HFMR_{\parallel}$ ($\mu_0 H = 0.73\text{ T}$) measured at 78 K and the characteristic coercive field $H_{c\parallel}$ estimated for various LSMO films at 78 K.

$T_s, ^\circ\text{C}$	$MR_{\parallel}(305\text{ K}), \%$	$MR_{\perp}^*(305\text{ K}), \%$	$LFMR_{\parallel}(78\text{ K}), \%$	$HFMR_{\parallel}(78\text{ K}), \%$	$\mu_0 H_{c\parallel}(78\text{ K}), \text{mT}$
800	-16	-	-0.3	-0.2	-
750	-8.0	-9.0	-5.4	-2.5	4.5
700	-7.0	-7.2	-7.9	-3.1	7.0
650	-3.0	-4.1	-10.2	-6.5	7.5
600	-2.0	-1.1	-10.5	-4.7	9.7
550	-0.3	-0.7	-14.1	-8.0	9.0

4. Discussion

The highest crystalline quality, i. e. highly (001)-plane oriented crystalline structure, has been identified in this work for the L800 film when grown by RF magnetron sputtering on MgO(001) single crystal substrate. This our finding is inconsistent with earlier report [23] certifying growth of high crystalline quality LSMO films on MgO(001) substrates at 800 °C in spite of large lattice mismatch ($\sim 8\%$). Resistivity versus temperature measurements also show high crystalline quality of the L800 film (see Fig. 3(a)). Certainly, a clearly defined resistance drop seen for the film with temperature decreasing below T_p ($\sim 330\text{ K}$) is typical of the highest quality epitaxial LSMO films when grown on SrTiO₃ and other lattice-matched substrates [2]. Therefore we conclude that a significant resistance drop seen for the film at $T < T_p$ related to the PM-FM phase transition at the Curie temperature ($T_c \cong T_p$) and the observed peak-like MR behaviour below T_p (the so-called CMR effect) represent intrinsic properties of highly (001)-plane oriented grains.

We associate enhanced resistivity of all LSMO films grown in this work at lower temperatures with high angle grain boundaries which may be formed between dominating (001)-oriented grains and a certain

relatively small amount of grains with (011) or other textures. We do believe that in the case of significant mismatch between LSMO and MgO lattice parameters high angle grain boundaries could be formed during early crystallization stages to reduce strains accommodated at the edges of (001)-plane oriented grains. High electrical resistance of these high angle grain boundaries may be caused by distorted chemical bonds, reduced crystallinity and occurrence of oxygen vacancies or other point defects in a close vicinity to the GBs. One can expect also that double exchange mechanism responsible for the ferromagnetic state might be suppressed at GBs giving rise to the appearance of highly resistive intergrain media [7].

The enhanced electrical resistivity of polycrystalline manganite film, $\rho(T)$, with current flowing via an array of grains and grain boundaries, can be understood by applying a simple quasi-linear 1D approximation [5]:

$$\rho(T) = \rho_G(T) + \left(\frac{d_{GB}}{d_G} \right) \rho_{GB}(T). \quad (1)$$

Here $\rho_G(T)$ and $\rho_{GB}(T)$ represent partial resistivity defined by grains and highly resistive GBs, d_G , d_{GB} are the averaged dimensions of grains and grain boundaries, respectively. It has been assumed for simplicity that $d_G \gg d_{GB}$.

It can be seen from Fig. 3(a) that resistivity of the L550 and L600 films at all temperatures is significantly higher compared to that of the L800 film. Therefore resistivity of these films should be defined mainly by the second term in (1) while the first term needs to be taken into account for the L750, L700 and L650 films demonstrating significantly lower resistivity values.

To reveal additional resistivity of polycrystalline LSMO films governed by GBs, in Fig. 6 we show the $\Delta\rho(T)$ plots obtained for various films by eliminating contribution of internal grain resistivity of the highest crystalline quality L800 film from the corresponding $\rho(T)$ curves displayed in Fig. 3(a). Presence of the characteristic maxima in the $\Delta\rho(T)$ plots with relatively low peak temperatures (T_p) may be associated with the PM-FM phase transition in the intergrain regions characterized by reduced carrier density compared to that inside the grains. Rather low T_p values seen in the $\Delta\rho(T)$ plots of the L600 and L550 films and semiconductor-like $\rho(T)$ behaviour observed for these films in a wide temperature range (down to T_p) may be understood assuming reduced carrier density in the intergrain region due to relatively low deposition temperatures. Certainly, lowering of the PM-FM transition temperature, T_C , with carrier density decreasing is known to be a common feature of all manganite films [1, 2].

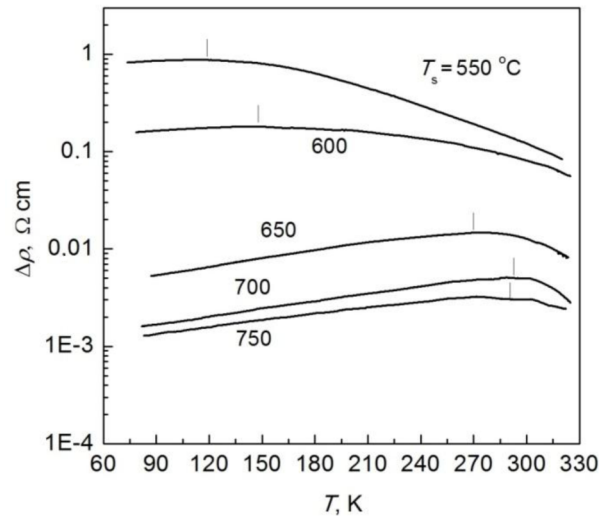


Fig. 6. Temperature-dependent additional resistivity of polycrystalline LSMO films, $\Delta\rho$, evaluated by eliminating internal resistivity of the highest crystalline quality L800 film from the corresponding $\rho(T)$ plots in Fig. 5(a).

Correlation of $\Delta\rho$ with the inverse grain size, $1/d_G$ (see Table 1), at $T = 300$ K and 78 K is shown in Fig. 7. Both gradual increase of the $\Delta\rho$ values with $1/d_G$ ($\Delta\rho \sim 1/d_G$) seen in Fig. 7 for the L750, L700 and L650 films with the largest grains and almost parallel shift of the $\Delta\rho(T)$ plots for the same films in Fig. 6 certify that in a wide range of deposition temperatures ($T_s = 650$ – 750 °C) $\Delta\rho$ depends mainly on the density of GBs. This experimental finding is inconsistent with similar data reported for polycrystalline LCMO films [4] when grown on polycrystalline substrates. Meanwhile significantly enhanced $\Delta\rho$ values indicated for fine-grain films grown at the lowest temperatures ($T_s = 600$ and 550 °C) demonstrate significant change of the additional resistivity with deposition temperature variation in the range 600–650 °C.

Specific GB-governed additional resistivity ($\Delta\rho \cdot d_G$) of about 10^{-8} Ω cm² (at $T = 78$ K) can be evaluated from Fig. 7 for the L750, L700 and L650 films exhibiting the highest grain size. Meanwhile, significantly higher values (of about 10^{-6} Ω cm² at $T = 78$ K) can be estimated from the same figure for the fine-grained films grown at $T \leq 650$ °C. The estimated values may be compared to the specific grain boundary resistivity of 2×10^{-5} Ω cm² reported earlier for polycrystalline $\text{La}_{0.7}\text{Ca}_{0.3}\text{MnO}_3$ (LCMO) films (at $T = 10$ K) [5] although significantly higher values (ranging from 10^{-2} to 1 Ω cm²) at $T \ll T_C$ have been found for the artificial GBs formed by growing the LCMO films on bicrystal substrates [7].

We turn now to the discussion of contribution of grains and grain boundaries to MR of the prepared

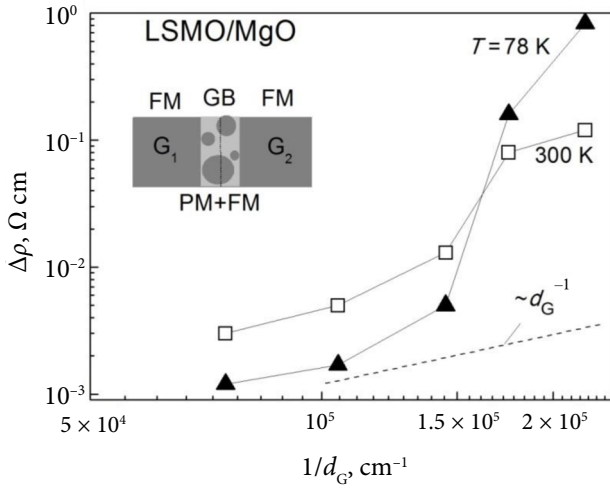


Fig. 7. The grain boundary-governed additional resistivity of various polycrystalline LSMO films at $T = 78$ and 300 K as a function of the inverse grain size, $1/d_G$. Simplified drawing of the GB model suggesting the phase separated state at GBs and possible carrier transport across GBs via two parallel channels is shown in the inset.

LSMO films. From (1) we get the following expression to estimate MR of a polycrystalline manganite film:

$$MR = \alpha MR_G + (1 - \alpha) MR_{GB}, \quad (2)$$

where MR_G and MR_{GB} are constituent parts of film magnetoresistance defined by grains and grain boundaries, respectively, and $\alpha = \rho_G/\rho$.

Let us concentrate in the beginning on high temperatures (just below T_C), where the highest negative CMR values of about 14% (at $T = 305$ K and $\mu_0 H_{||} = 0.73$ T) have been measured for the L800 film. It has been pointed out earlier that magnetoresistance defined by grain boundaries in both polycrystalline ceramics and LSMO thin films is the highest at low temperatures while the MR_{GB} reduces down to negligibly small values at room temperature [2, 10, 13, 23]. Therefore the first term in (2) is dominating and MR of polycrystalline LSMO films at room and higher temperatures below T_C should be defined mainly by grains rather than by GBs. It can be seen from (2) also that MR of polycrystalline films containing highly resistive GBs should be reduced compared to that of the highest quality L800 film by the factor $\alpha = \rho_G/\rho$ (< 1).

The MR values estimated for all polycrystalline LSMO films at $T = 305$ K from (2) referred to as $MR^*(305$ K) are displayed in Table 2. The highest intrinsic magnetoresistance of grains (MR_G) of -14% measured for the L800 film at 305 K has been used for the estimation while the α values for various polycrystalline films were obtained from the correspond-

ing $\rho(T)$ plots in Fig. 3(a) assuming for simplicity that grain resistivity of all polycrystalline films at 305 K is the same as that of the L800 film ($\rho_G = 6.0$ m Ω cm). Taking into account good coincidence of the estimated $MR^*(305$ K) values with the corresponding $MR(305$ K) data measured directly (see Table 2) we conclude that magnetoresistance of polycrystalline LSMO films at high temperatures (just below T_C) is defined mainly by the intrinsic CMR effect of grains. We certify also that a role of grains in MR of polycrystalline LSMO films at room and higher temperatures ($T < T_C$) is reduced due mainly to a significant (magnetic field independent) series resistance of GBs.

At low temperatures, i. e. at $T = 78$ K ($\ll T_C$), one can notice in Fig. 3(a, b) that $\rho \gg \rho_G$ and $|MR_G| \ll |MR_{GB}|$ for all polycrystalline LSMO films prepared in this work. So, we conclude that at $T = 78$ K the first term in (2) can be neglected and MR of all the grown polycrystalline LSMO films at low temperatures should be defined mainly by GBs.

To explain the LFMR effect indicated in this work for polycrystalline LSMO films at low temperatures (see Fig. 5) we concentrate on the most widely accepted model based on tunnelling of spin-polarized carriers between neighbouring ferromagnetic grains [7, 13]. It can be seen from Fig. 5 that clearly defined peak-like $\rho(H)$ anomalies at low fields have been indicated for all polycrystalline LSMO films although their resistivity varied in a surprisingly wide range and they demonstrated different $\rho(T)$ behaviour (either metallic or semiconductor-like). So, following the proposed tunnelling model we are forced to assume the presence of sharp GBs acting as high quality tunnel junctions with an ultrathin (~ 1 – 3 nm) barrier and the adjacent FM electrodes exhibiting spin-polarized carriers for all polycrystalline LSMO films independently on their resistivity.

It is important to note, however, that semiconductor-like $\rho(T)$ behaviour indicated for the L550 and L600 films in a wide temperature range cannot be accounted for within the tunnelling model [7]. Certainly, high resistivity values and $\rho(T)$ relations measured for the films show unambiguously the formation of highly resistive regions with reduced carrier density at GBs. Therefore semiconductor-like $\rho(T)$ behaviour observed for the films may be understood assuming hopping carrier transport via the intergrain regions [10]. At the same time, magnetoresistive properties of GBs measured for the films at high fields, i. e. the HFMR effect, may be ascribed to an alignment of disordered spins in the intergrain regions (with lower magnetic order and reduced density of carriers) under the applied magnetic field favouring hopping carrier transport and thus reducing the GB resistance [17].

Complex magnetotransport properties of GBs in the prepared LSMO films, i. e. coexistence of the LFMR and HFMR effects, may be easily understood following the concept of spatially nonuniform current flow across the GBs via coexisting low and high conductivity channels [10, 18, 19, 25]. We associate the presence of two kinds of conductivity channels at GBs with the well-known phase separation phenomenon in doped manganites [2, 26]. Thermodynamic modelling of phase separation in manganites predicts two kinds of phase separation scenario: a) electronic phase separation leading to coexisting clusters of a nanometre scale with high and low carrier densities and b) disorder-induced phase separation with percolative characteristics of the FM clusters with a typical size up to $1.0 \mu\text{m}$ embedded in a highly resistive paramagnetic (PM) matrix. [2, 27]. Importance of the phase separation phenomenon leading to coexistence of the highly resistive PM phase with the metallic FM phase has been manifested by a number of authors to explain complex transport properties of polycrystalline manganites [1, 28, 29].

We do believe that the most favourable conditions for the phase-separated state in the grown LSMO films could be realized at GBs due to a number of factors such as reduced carrier density, nonuniform strains caused by a substrate and possible microscopic structural nonhomogeneities [2, 27]. Taking into account reduced carrier density in the intergrain region, it is natural to expect that the FM state in the vicinity of GBs at $T < T_C$ appears in a form of FM clusters with a fixed carrier density embedded in the highly resistive PM matrix. Schematic drawing of a single GB (at $T < T_C$) demonstrating coexistence of highly conductive (FM) and highly resistive (PM) regions at the interface between the adjacent misoriented FM grains G1 and G2 is shown in the inset to Fig. 7.

Following the simplified model of GB one can expect that spin-polarized tunnelling of carriers across GBs may only be realised via the FM regions located in front of each other at both sides of the interface. The LFMR effect may be easily understood taking into account current flowing in the conductive channel, i. e. via the conductive FM regions and a certain partial square (S_{tunn}) of the FM-I-FM tunnel junction. Similarity of peak-like *MR* anomalies at low magnetic field seen in Fig. 3(b) for the L750, L650 and L550 films exhibiting different resistivity (see Fig. 3(a)) can be understood assuming that carrier density in phase separated FM regions of various films is almost the same although partial volume of the FM phase regions is significantly reduced with deposition temperature decreasing.

Finally, *MR* of the grown polycrystalline LSMO films at high fields (HFMR effect) could be associated with magnetic field-driven hopping of carriers across the GBs and the adjacent highly resistive PM regions. Note also that *MR* of GBs at high magnetic fields could depend additionally on the magnetic field-driven partial volume of the FM phase in phase-separated material at GBs.

4. Conclusions

LSMO thin films exhibiting a highly (001)-plane oriented and polycrystalline structure have been grown by magnetron sputtering on MgO(001) single crystal substrates at $T = (550\text{--}800) \text{ }^\circ\text{C}$. Competing contribution of grains and grain boundaries on temperature-dependent resistivity and magnetoresistance of the films has been elucidated. The highest negative *MR* values up to 14% at 300 K under magnetic field $\mu_0 H_{\parallel} = 0.73 \text{ T}$ have been measured for highly oriented L800 films. Reduced *MR* values measured for all polycrystalline LSMO films (at 300 K) have been explained assuming additional magnetic field independent series resistance of grain boundaries.

Our investigations revealed the key importance of grain boundaries in polycrystalline LSMO films on both increased resistivity values and magnetoresistance at low temperatures. A model based on two parallel channels of carrier transport across grain boundaries has been used to explain coexistence of the LFMR and HFMR effects for polycrystalline LSMO films at low temperatures. The LFMR effect has been explained assuming tunneling of spin-polarized carriers via tunnelling barriers formed naturally between misoriented grains, while significant HFMR values measured for the films at $T \ll T_C$ have been associated with magnetic field-dependent hopping of carriers via the intergrain regions with reduced carrier density. We point out the key importance of the phase separation phenomenon for both microstructure of GBs and the resultant GB-governed complex magnetotransport phenomena in thin films of polycrystalline manganites.

References

- [1] M. Ziese, Extrinsic magnetotransport phenomena in ferromagnetic oxides, Rep. Prog. Phys. **65**, 143–249 (2002), <http://dx.doi.org/10.1088/0034-4885/65/2/202>
- [2] P.K. Siwach, H.K. Singh, and O.N. Srivastava, Low field magnetotransport in manganites, J. Phys. Condens. Matter **20**, 273201 (43pp) (2008), <http://dx.doi.org/10.1088/0953-8984/20/27/273201>

- [3] L. Balcells, J. Fontcuberta, B. Martínez, and X. Obradors, High-field magnetoresistance at interfaces in manganese perovskites, *Phys. Rev. B* **589**(22), R14697–147000 (1998), <http://dx.doi.org/10.1103/PhysRevB.58.R14697>
- [4] M. Ziese, Grain-boundary magnetoresistance in manganites: Spin-polarized inelastic tunneling through a spin-glass-like barrier, *Phys. Rev. B* **60**(2), R738–741 (1999), <http://dx.doi.org/10.1103/PhysRevB.60.R738>
- [5] A. Gupta, G.Q. Gong, G. Xiao, P.R. Duncombe, P. Lecoeur, P. Trouilloud, Y.Y. Wang, V.P. Dravid, and J.Z. Sun, Grain-boundary effects on the magnetoresistance properties of perovskite manganite films, *Phys. Rev. B* **54**(22), R15629–15632 (1996), <http://dx.doi.org/10.1103/PhysRevB.54.R15629>
- [6] M. Paranjape, J. Mitra, A.K. Raychaudhuri, N.K. Todd, N.D. Mathur, and M.G. Blamire, Nonlinear electrical transport through artificial grain-boundary junctions in $\text{La}_{0.7}\text{Ca}_{0.3}\text{MnO}_3$ epitaxial thin films, *Phys. Rev. B* **68**, 144409 (2003), <http://dx.doi.org/10.1103/PhysRevB.68.144409>
- [7] R. Gross, L. Alff, B. Buchner, B.H. Freitag, C. Hofener, J. Klein, Y. Lu, W. Mader, J.B. Philipp, M.S.R. Rao, P. Reutler, S. Ritter, S. Thienhaus, B. Uhlenbruck, and B. Wiedenhorst, Physics of grain boundaries in the colossal magnetoresistance manganites, *J. Magn. Magn. Mater.* **211**, 150–159 (2000), [http://dx.doi.org/10.1016/S0304-8853\(99\)00727-1](http://dx.doi.org/10.1016/S0304-8853(99)00727-1)
- [8] J. Rivas, L.E. Hueso, A. Fondado, F. Rivadulla, and M.A. Lopez-Quintela, Low field magnetoresistance effects in fine particles of $\text{La}_{0.67}\text{Ca}_{0.33}\text{MnO}_3$ perovskites, *J. Magn. Magn. Mater.* **221**, 57–62 (2000), [http://dx.doi.org/10.1016/S0304-8853\(00\)00384-X](http://dx.doi.org/10.1016/S0304-8853(00)00384-X)
- [9] P.K. Muduli, G. Singh, R. Sharma, and R.C. Budhani, Magnetotransport in polycrystalline $\text{La}_{2/3}\text{Sr}_{1/3}\text{MnO}_3$ thin films of controlled granularity, *J. Appl. Phys.* **105**, 113910 (2009), <http://dx.doi.org/10.1063/1.3124372>
- [10] J.-M. Liu, G.L. Yuan, Q. Huang, J. Li, Z.G. Liu, and Y.W. Du, The effect of the deposition temperature on the low-field magnetoresistance of polycrystalline $\text{La}_{0.5}\text{Sr}_{0.5}\text{MnO}_3$ thin films produced by pulsed laser deposition, *J. Phys. Condens. Matter* **13**, 11–23 (2001), <http://iopscience.iop.org/0953-8984/13/1/302>
- [11] S. Ju, H. Sun, and Z.Y. Li, Study of magnetotransport in polycrystalline perovskite manganites, *J. Phys. Condens. Matter* **14**, L631–L639 (2002), <http://dx.doi.org/10.1088/0953-8984/14/38/102>
- [12] M. Julliere, Tunneling between ferromagnetic films, *Phys. Lett. A* **54**(3), 225–226 (1975), [http://dx.doi.org/10.1016/0375-9601\(75\)90174-7](http://dx.doi.org/10.1016/0375-9601(75)90174-7)
- [13] H.Y. Hwang, S.-W. Cheong, N.P. Ong, and B. Batlogg, Spin-polarized intergrain tunneling in $\text{La}_{2/3}\text{Sr}_{1/3}\text{MnO}_3$, *Phys. Rev. Lett.* **77**(10), 2041–2044 (1996), <http://dx.doi.org/10.1103/PhysRevLett.77.2041>
- [14] J.E. Evetts, M.G. Blamire, N.D. Mathur, S.P. Isaac, B.S. Teo, L.F. Cohen, and J.L. Macmanus-Driscoll, Defect-induced spin disorder and magnetoresistance in single-crystal and polycrystal rare-earth manganite thin films, *Phil. Trans. R. Soc. Lond. A* **356**, 1593–1615 (1998), <http://dx.doi.org/10.1098/rsta.1998.0237>
- [15] S. Ju, K.W. Yu, and Z.Y. Li, Theory of ingranular magnetoresistance in nanometric manganites, *Phys. Rev. B* **71**, 014416 (2005), <http://dx.doi.org/10.1103/PhysRevB.71.014416>
- [16] R. Gunnarsson, A. Kadigrobov, and Z. Ivanov, Model for spin-polarized transport in perovskite manganite bicrystal grain boundaries, *Phys. Rev. B* **66**, 024404 (2002), <http://dx.doi.org/10.1103/PhysRevB.66.024404>
- [17] N. Zurauskiene, S. Balevicius, P. Cimpmperman, V. Stankevic, S. Kersulis, J. Novickij, A. Abrutis, and V. Plausinaitiene, Colossal magnetoresistance of $\text{La}_{0.83}\text{Sr}_{0.17}\text{MnO}_3$ thin films grown by MOCVD on lucalox substrate, *J. Low Temp. Phys.* **159**, 64–67 (2010), <http://dx.doi.org/10.1007/s10909-009-0073-y>
- [18] A. de Andres, M. Garcia-Hernandez, and J.L. Martinez, Conduction channels and magnetoresistance in polycrystalline manganites, *Phys. Rev. B* **60**(10), 7328–7334 (1999), <http://dx.doi.org/10.1103/PhysRevB.60.7328>
- [19] A. de Andres, M. Garcia-Hernandez, J.L. Martinez, and C. Prieto, Low-temperature magnetoresistance in polycrystalline manganites: connectivity versus grain size, *Appl. Phys. Lett.* **74**(25), 3884–3886 (1999), <http://dx.doi.org/10.1063/1.124212>
- [20] S. Mercone, C.A. Perroni, V. Cataudella, C. Adamo, M. Angeloni, C. Aruta, G. De Filippis, F. Miletto, A. Oropallo, P. Perna, A. Yu. Petrov, U. Scotti di Uccio, and L. Maritato, Transport properties in manganite thin films, *Phys. Rev. B* **71**, 064415 (2005), <http://arxiv.org/abs/cond-mat/0410743>
- [21] M. Egilmez, R. Patterson, K.H. Chow, and J. Jung, Magnetoresistive anisotropy and magnetoresistivity in strained $\text{La}_{0.65}\text{Ca}_{0.35}\text{MnO}_3$ films near the metal-insulator transition, *Appl. Phys. Lett.* **90**, 232506 (2007), <http://dx.doi.org/10.1063/1.2746956>
- [22] R. Gunnarsson and M. Hanson, Magnetization reversal processes in magnetic bicrystal junctions, *Phys. Rev. B* **73**, 014435 (2006), <http://dx.doi.org/10.1103/PhysRevB.73.014435>
- [23] M. Spankova, S. Chromik, I. Vavra, K. Sedlackova, P. Lobotka, S. Lucas, and S. Stancek, Epitaxial LSMO films grown on MgO single crystalline substrates, *Appl. Surf. Sci.* **253**, 7599–7603 (2007), <http://dx.doi.org/10.1016/j.apsusc.2007.03.058>
- [24] P. Raychaudhuri, K. Sheshadri, P. Taneja, S. Bandyopadhyay, P. Ayyub, A.K. Nigam, and R. Pinto, Spin-polarized tunneling in the half-metallic

- ferromagnets $\text{La}_{0.7-x}\text{Ho}_x\text{Sr}_{0.3}\text{MnO}_3$ ($x = 0$ and 0.15): Experiment and theory, Phys. Rev. B **59**(21), 13919–13926 (1999), <http://dx.doi.org/10.1103/PhysRevB.59.13919>
- [25] A. Chen, W. Zhang, J. Jian, H. Wang, C.F. Tsai, Q. Su, Q. Sia, and J.L. MacManus-Driscoll, Role of boundaries on low-field magnetotransport properties of $\text{La}_{0.7}\text{Sr}_{0.3}\text{MnO}_3$ -based nanocomposite thin films, J. Mater. Res. **28**(13), 1707–1714 (2013), <http://dx.doi.org/10.1557/jmr.2013.89>
- [26] E. Dagotto, T. Hotta, and A. Moreo, Phys. Rep. **344**, 1 (2001), [http://dx.doi.org/10.1016/S0370-1573\(00\)00121-6](http://dx.doi.org/10.1016/S0370-1573(00)00121-6)
- [27] J. Sacanell, F. Parisi, J.C.P. Campoy, and L. Ghivelder, Thermodynamic modeling of phase separation in manganites, Phys. Rev. B **73**, 014403 (2006), <http://dx.doi.org/10.1103/PhysRevB.73.014403>
- [28] M. Bibes, L. Balcells, S. Valencia, J. Fontcuberta, M. Wojcik, E. Jedryka, and S. Nadolski, Phys. Rev. Lett. **87**, 067210 (2001), <http://dx.doi.org/10.1103/PhysRevLett.87.067210>
- [29] M.H. Jo, N.D. Mathur, N.K. Todd, and M.G. Blamire, Very large magnetoresistance and coherent switching in half-metallic manganite tunnel junctions, Phys. Rev. B **61**(22), R14905 (2000), <http://dx.doi.org/10.1103/PhysRevB.61.R14905>

PLONŪJŲ TEKSTŪRUOTŲ IR POLIKRISTALINIŲ $\text{La}_{0.67}\text{Sr}_{0.33}\text{MnO}_3/\text{MgO}(001)$ SLUOKSNIŲ ELEKTRINĖ VARŽA IR MAGNETOVARŽA

B. Vengalis^a, I. Černiukė^a, A. Maneikis^a, A.K. Oginskis^a, G. Grigaliūnaitė-Vonsevičienė^b

^a *Fizinių ir technologijos mokslų centras, Vilnius, Lietuva*

^b *Vilniaus Gedimino technikos universitetas, Vilnius, Lietuva*

Santrauka

Plonieji (100) plokštumoje orientuoti $\text{La}_{0.67}\text{Sr}_{0.33}\text{MnO}_3$ (LSMO) sluoksniai, taip pat polikristaliniai LSMO sluoksniai su papildomais (110) plokštumoje orientuotais kristalitais buvo užauginti magnetroninio dulkinimo būdu keičiant kristalinių $\text{MgO}(100)$ padėklų temperatūrą nuo 550 iki 800 °C. Ištirta kristalinių grūdų ir tarpkristalinių sričių įtaka sluoksnių elektrinei varžai ir magnetovaržai 78–330 K temperatūrų ruože. Tarpkristalinių ribų magnetovaržai silpnuose (LFMR) ir stipriuose (HFMR) magnetiniuose laukuose paaiškinti buvo pasitelktas dviejų lygiagrečių elektrai laidžių kanalų modelis. LFMR reiškinys polikristaliniuose

LSMO sluoksniuose paaiškintas krūvininkų su orientuotais sukiniais tuneliavimu per magnetiniu lauku valdomą tunelinį barjerą, susidarantį technologinio proceso metu tarp gretimų skirtingai orientuotų kristalinių grūdų. Žymi polikristalinių sluoksnių magnetovarža, esant žemoms temperatūroms ir stipriems magnetiniams laukams, buvo susieta su šuoliniu krūvininkų transportu per tarpkristalines sritis, pasižyminčias sumažinta krūvininkų koncentracija. Aptarta galima fazinio išsisluoksniavimo reiškinio įtaka nevienalytei tarpgrūdinei terpei susidaryti tiriamuosiuose polikristaliniuose LSMO sluoksniuose.